

210670: staurolite-bearing garnet pelitic schist, Lennard River (*Marboo Formation, Western Zone, Lamboo Province, Wunaamin Miliwundi Orogen*)

Korhonen, FJ, Romano, SS, Fielding, IOH, Kelsey, DE and Hollis, JA

Location and sampling

LENNARD RIVER (SE 51-8), RICHENDA (3963)

MGA Zone 51, 714401E 8074315N

WAROX site JBHLEN000199

Sampled on 26 June 2013

This sample was collected from an outcrop on Napier Downs Station, about 10.0 km west-southwest of Mount Joseph, 4.9 km east of Windjana Gorge, and 1.3 km north of the Lennard River.

Geological context

The unit sampled is a pelitic schist assigned to the Marboo Formation of the Lamboo Province. The 1872–1864 Ma Marboo Formation is the oldest rock unit in the Lamboo Province, which forms an elongate belt of deformed and metamorphosed Paleoproterozoic sedimentary and igneous rocks (Tyler et al., 1999; 2012; Maidment et al., 2022). The Marboo Formation is a succession of turbiditic metasedimentary rocks with paleocurrent directions implying derivation from the northwest in an area of crust now buried beneath the unconformably overlying Speewah and Kimberley Basins (Tyler et al., 1999). The sample at this locality was collected within the northwest-trending Billyarra Shear Zone. A pelitic schist of the Marboo Formation, sampled about 16.5 km to the northwest, yielded a maximum depositional age of 1874 ± 5 Ma for the sedimentary protolith (GSWA 212344, Lu et al., 2016). West-northwest-directed folding and thrusting and shear zone reactivation occurred during the 670–510 Ma Wunaamin Miliwundi Orogeny (formerly the King Leopold Orogeny; Tyler and Griffin, 1990; Tyler et al., 2012). Monazite in the sample reported here yield a date of 502 ± 3 Ma (Fielding et al., 2019b), many of which are aligned in the foliation. Rb–Sr isochron ages from muscovite in this sample yielded similar dates (GSWA 210670, preliminary data). In situ Lu–Hf dates of garnet cores and rims from this sample are within uncertainty and yield an isochron age of c. 559 Ma (GSWA 210670, preliminary data). Monazites in pelitic schists of the Marboo Formation, sampled about 0.3 km northwest and 1.1 km east-southeast of the present sample, yield dates of 505 ± 5 Ma (GSWA 210664, Fielding et al., 2019a) and 501 ± 3 Ma (GSWA 210671, Fielding et al., 2019c). These dates are younger than K–Ar ages of c. 560 Ma from reactivated shear zones in the Halls Creek Orogen in the west Kimberley (Shaw et al., 1992), and are interpreted to represent the age of deformation and metamorphism during the final stages of the Wunaamin Miliwundi Orogeny.

Petrographic description

The sample is a pelitic schist (Fig. 1), consisting of about 40% muscovite, 38% quartz, 10% garnet, 6% chlorite, 4% biotite, 2% staurolite, trace ilmenite and magnetite, and accessory monazite and apatite (Fig. 2; Table 1). Garnet and staurolite porphyroblasts occur within a strongly foliated, fine-grained groundmass of muscovite, quartz, chlorite, biotite, ilmenite, and monazite. In some places the foliation is crenulated. Garnet porphyroblasts are up to 1.5 cm in size and contain sigmoidal inclusion trails dominated by quartz, with trace ilmenite, muscovite, tourmaline, and apatite (Fig. 3a,b). In some porphyroblasts the sigmoidal fabric is continuous with the main foliation (Figs 2, 3a). Some smaller garnets are inclusion-poor, and garnet rims with fewer inclusions occur in many grains that locally truncate the inclusion trails (Figs 2, 3b). Staurolite porphyroblasts are up to 8 mm long, although most are less than 4 mm, and contain inclusions of ilmenite, quartz and biotite that are aligned and continuous with the main foliation (Fig. 3c). Chlorite laths are oriented both parallel and oblique to the foliation (Fig. 3d), and chlorite also fills fractures within garnet, surrounds staurolite, and forms rare coarse clots within the matrix. Brown biotite occurs as laths up to 1 mm long within the foliation and rare discrete subhedral porphyroblasts (Fig. 3d).



Figure 1. Outcrop image for sample 210670: staurolite-bearing garnet pelitic schist, Lennard River

Table 1. Mineral modes for sample 210670: staurolite-bearing garnet pelitic schist, Lennard River

Mineral modes	Grt	St	Bt	Ms	Chl	Pl	Qz	Ilm	Mag
Observed (vol%)	10	2	4	40	6	–	38	trace	trace
Predicted (mol%)									
@ 6 kbar, 600 °C	0.2	6.0	8.9	28.3	–	3.0	51.8	1.3	0.6
@ 6 kbar, 625 °C	0.1	6.7	8.8	26.8	–	4.0	51.8	1.2	0.7
@ 7 kbar, 625 °C	0.9	5.8	8.1	28.8	–	3.0	51.5	1.3	0.5
@ 7 kbar, 650 °C	0.6	6.6	8.1	27.2	–	4.1	51.5	1.3	0.6

NOTES: – not present

Analytical details

The metamorphic evolution of this sample was investigated using phase equilibria, based on the bulk-rock composition (Table 2). The composition was determined by X-ray fluorescence spectroscopy, together with loss on ignition (LOI). FeO content was analysed by Fe^{2+} titration, and Fe_2O_3 calculated by difference. The O content (for Fe^{3+}) was initially based on the Fe_2O_3 :FeO proportion determined by titration (= 47% Fe as Fe^{3+}). However, the models failed due to difficulties in calculating the solvus along the ilmenite–hematite binary for this composition. In order to resolve these issues, the Fe_2O_3 :FeO proportion was reduced slightly from 47% Fe as Fe^{3+} to 37% Fe as Fe^{3+} , which yield results consistent with the observed equilibria. The subsolidus mineral assemblages are assumed to have equilibrated in the presence of a pure H_2O volatile fluid; therefore, the calculations were performed in an H_2O -saturated system. Thermodynamic calculations were performed in the MnNCKFMASHTO (MnO – Na_2O – CaO – K_2O – FeO – MgO – Al_2O_3 – SiO_2 – H_2O – TiO_2 –O) system using THERMOCALC version tc340 (updated October 2013; Powell and Holland, 1988) and the internally consistent thermodynamic dataset of Holland and Powell (2011; dataset tc-ds62, created in February 2012). The activity–composition relations used in the modelling are detailed in White et al. (2014a,b). Compositional and mode isopleths for all phases were calculated using the software TCIInvestigator (Pearce et al., 2015). Additional information on the workflow with relevant background and methodology are provided in Korhonen et al. (2020).

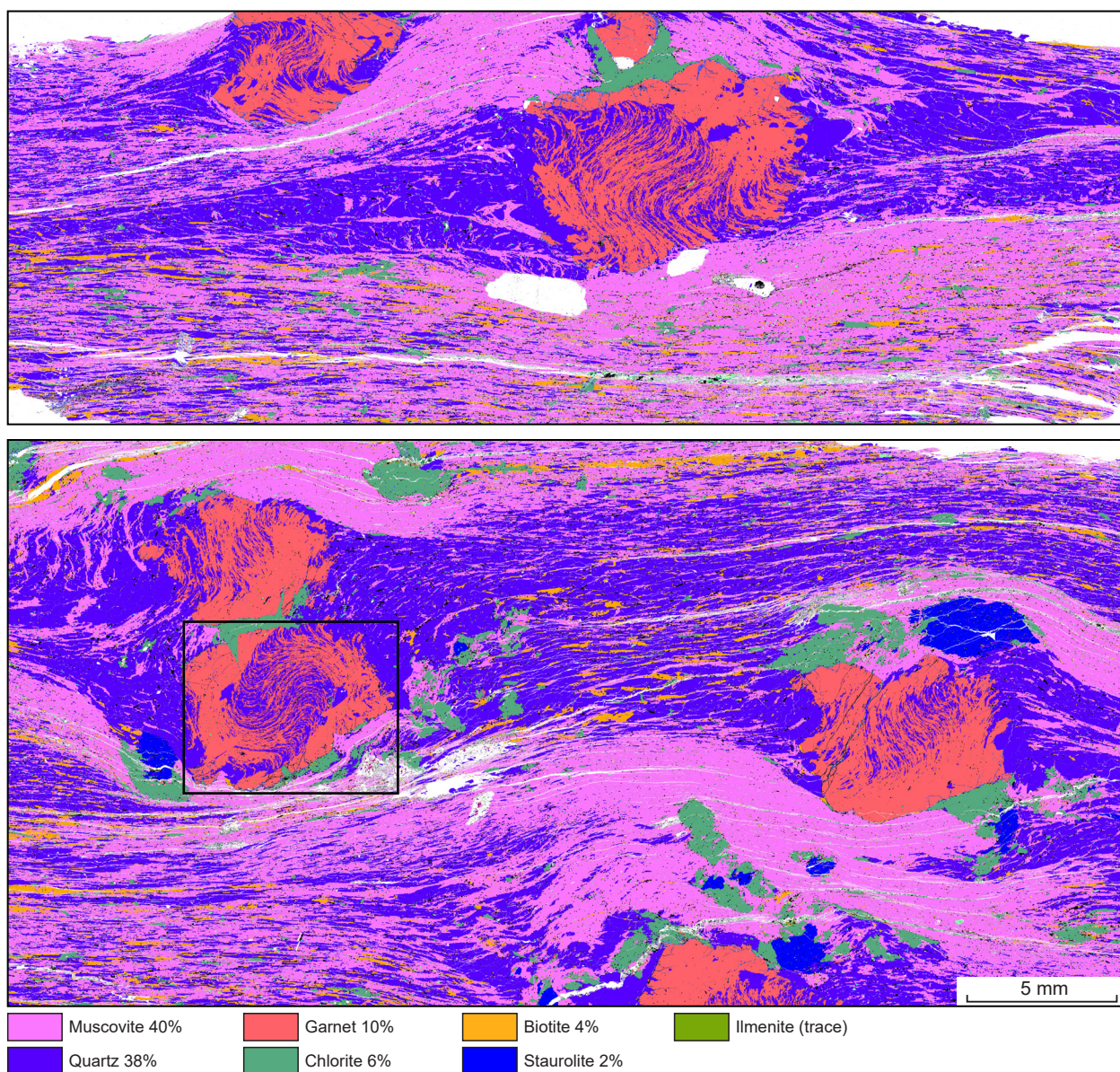


Figure 2. TESCAN Integrated Mineral Analyser (TIMA) image of an entire thin section from sample 210670: staurolite-bearing garnet pelitic schist, Lennard River. Volume percent proportions of major rock-forming minerals are calculated by the TIMA software. White pixels denote holes. Black rectangle shows location of electron probe microanalyser (EPMA) garnet map (Appendix 2)

Table 2. Measured whole-rock and modelled compositions for sample 210670: staurolite-bearing garnet pelitic schist, Lennard River

<i>XRF whole-rock composition (wt%)(a)</i>											
SiO ₂	TiO ₂	Al ₂ O ₃	Fe ₂ O ₃ ^(b)	FeO ^(b)	MnO	MgO	CaO	Na ₂ O	K ₂ O	LOI	Total
69.70	0.57	15.66	2.85	2.83	0.07	1.23	0.31	0.68	3.31	2.16	99.37
<i>Normalized composition used for phase equilibria modelling (mol%)</i>											
SiO ₂	TiO ₂	Al ₂ O ₃	O ^(c)	FeO ^{T(d)}	MnO	MgO	CaO	Na ₂ O	K ₂ O	H ₂ O ^(e)	Total
77.71	0.48	10.29	0.93	5.03	0.07	2.05	0.37	0.74	2.35	excess	100

NOTES: (a) Data and analytical details are available from the WACHEM database <<http://geochem.dmp.wa.gov.au/geochem/>>
(b) FeO analysed by Fe²⁺ titration; Fe₂O₃ content calculated by difference
(c) O content (for Fe³⁺) slightly reduced from titration value; see text
(d) FeO^T = moles FeO + 2 * moles O
(e) H₂O-saturated

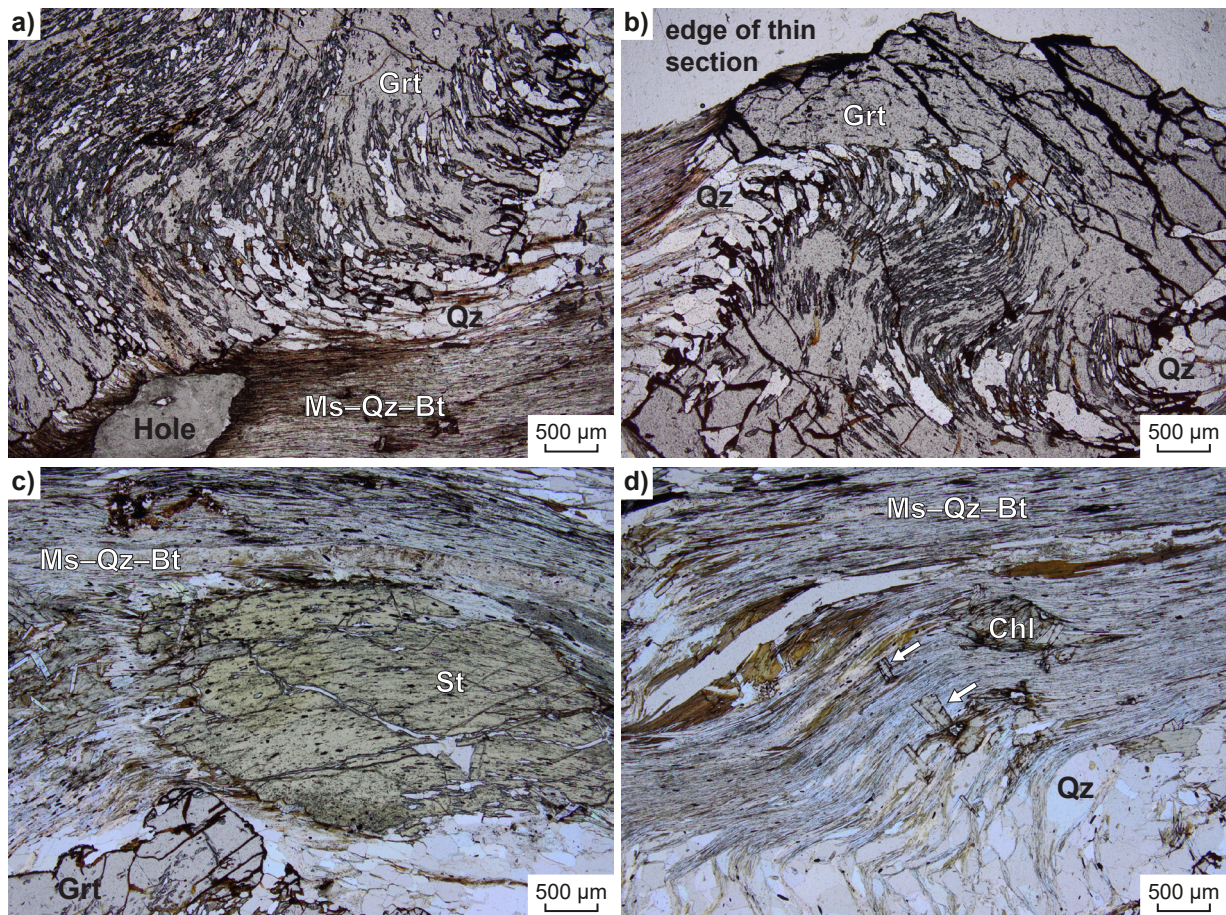


Figure 3. Photomicrographs in plane-polarized light of sample 210670: staurolite-bearing garnet pelitic schist, Lennard River. White arrows in (d) point to chlorite. Abbreviations: Bt, biotite; Chl, chlorite; Grt, garnet; Ms, muscovite; Qz, quartz; St, staurolite

Results

Metamorphic P - T estimates have been derived based on detailed examination of two thin sections and the bulk-rock composition (Table 2). Care was taken to ensure that the thin section and the sample volume selected for whole-rock chemistry were similar in terms of featuring the same minerals in approximately the same abundances, to minimize any potential compositional differences. The P - T pseudosection for this sample was calculated over a P - T range of 2–9 kbar and 500–700 °C (Fig. 4). The H_2O -saturated solidus is stable between 665 and 700 °C over the range of modelled pressures. The sample did not undergo melting; therefore, equilibria were not modelled above the solidus. The pseudosection predicts typical Barrovian index minerals, with chlorite stable at temperatures below 520 °C, followed by the appearance of garnet, biotite, staurolite, and aluminosilicate with increasing temperature. Margarite is predicted to be stable between 515 and 635 °C above 5 kbar, although it been recognized to be overstabilized in metapelitic bulk compositions (e.g. Palin et al., 2016). Epidote-bearing assemblages are stable above 4 kbar between 500 and 565 °C, and plagioclase-absent assemblages are predicted above 4 kbar between 500 and 650 °C.

Mineral compositions are provided in Appendix 1 as an accompanying electronic file. Garnet porphyroblasts are almandine-rich and strongly zoned (Appendices 1, 2), with a progressive increase in $p(\text{Alm})$ [= $\text{Fe}^{2+}/(\text{Fe}^{2+} + \text{Mg} + \text{Ca} + \text{Mn})$] and $p(\text{Pyp})$ [= $\text{Mg}/(\text{Fe}^{2+} + \text{Mg} + \text{Ca} + \text{Mn})$] and a decrease in $X\text{Fe}$ [= $\text{Fe}^{2+}/(\text{Fe}^{2+} + \text{Mg})$], $p(\text{Grs})$ [= $\text{Ca}/(\text{Fe}^{2+} + \text{Mg} + \text{Ca} + \text{Mn})$], and $p(\text{Sps})$ [= $\text{Mn}/(\text{Fe}^{2+} + \text{Mg} + \text{Ca} + \text{Mn})$] from core to rim. Garnet cores have $X\text{Fe} = 0.93 - 0.94$, $p(\text{Alm}) = 0.69 - 0.72$, $p(\text{Grs}) = 0.18 - 0.19$, and $p(\text{Sps}) = 0.08 - 0.09$; rims have $X\text{Fe} = 0.90 - 0.92$; $p(\text{Alm}) = 0.82 - 0.83$, $p(\text{Grs}) = 0.07 - 0.08$, and no MnO. Staurolite is Fe-rich with $X\text{Fe} = 0.84 - 0.86$ and Zn cations per formula unit (pfu) between 0.16 and 0.31. Biotite is Fe-rich ($X\text{Fe} = 0.51 - 0.57$) and has TiO_2 wt% 1.34 – 1.75 (0.08 – 0.10 cations pfu). Fluorine ions in biotite are 0.14 – 0.19 ions pfu (11 oxygen basis), with negligible chlorine. Muscovite has paragonite content of 0.22 – 0.29, and negligible margarite. Chlorite is moderately Fe-rich, with $X\text{Fe}$ ratios of 0.53 – 0.55.

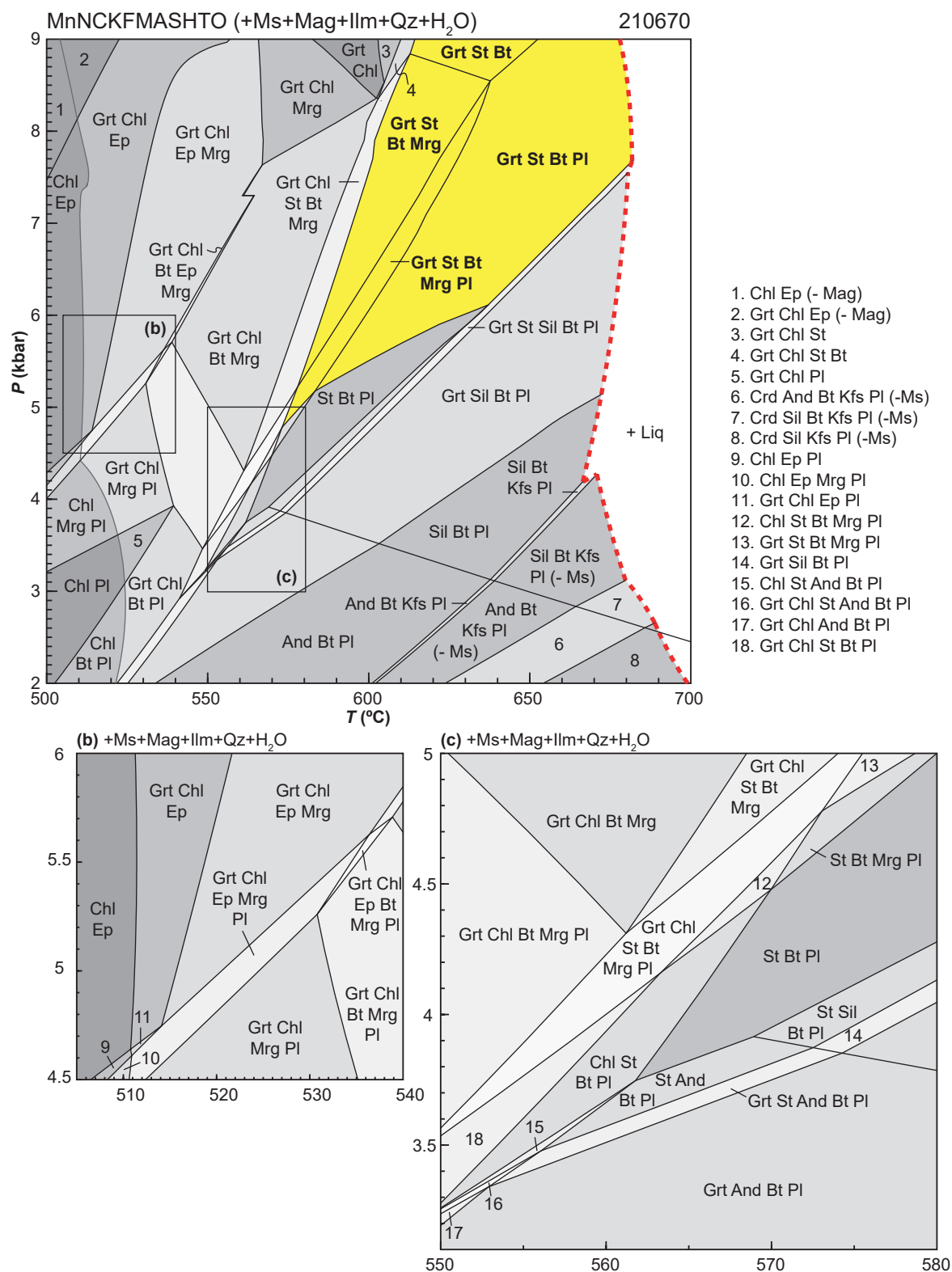


Figure 4. *P-T* pseudosection calculated for sample 210670: staurolite-bearing garnet pelitic schist, Lennard River. Assemblage field corresponding to peak metamorphic conditions is shown in bold text and yellow shading. Red dashed line represents the solidus. Abbreviations: And, andalusite; Bt, biotite; Chl, chlorite; Crd, cordierite; Ep, epidote; Grt, garnet; Ilm, ilmenite; Kfs, K-feldspar; Liq, silicate melt; Mag, magnetite; Mrg, margarite; Ms, muscovite; Pl, plagioclase; Qz, quartz; Sil, sillimanite; St, staurolite

Interpretation

Garnet is interpreted to have grown during progressive non-coaxial shear deformation, with growth of garnet and staurolite contemporaneous with development of the foliation. Based on these observations, the peak metamorphic assemblage is interpreted to include garnet, staurolite, biotite, muscovite, quartz, ilmenite and magnetite. Chlorite texturally appears to be associated with the breakdown of garnet and staurolite, and is interpreted to be a retrograde mineral. The inferred peak assemblage comprising garnet–staurolite–biotite–muscovite–magnetite–ilmenite–quartz (+H₂O) is predicted to be stable with margarite and/or plagioclase, with up to 2 mol% (molar proportions approximately equivalent to vol%) margarite and 4 mol% plagioclase in these fields (Appendix 3). Neither of these minerals are observed in the sample, which could be due to their consumption on the post-peak *P–T* path, or more likely the calculations overstabilize margarite. The peak field(s) have a stability field between 575 and 680 °C at a minimum pressure of 4.8 kbar (Fig. 4). The garnet–staurolite–biotite–muscovite–magnetite–ilmenite–quartz (+H₂O) field is predicted to be stable at unrealistically high pressures (>13 kbar; not shown), therefore the equilibria only provide a minimum pressure constraint. The peak field is delimited by the solidus at higher temperatures, and the stability of chlorite and the absence of staurolite at lower temperature. The lower pressure limit is defined by the absence of garnet and staurolite, and the stability of sillimanite.

The chemical zoning preserved in the garnet porphyroblasts is consistent with prograde growth. Calcium diffuses more slowly in garnet than the other major components (e.g. Carlson, 2006), and may preserve a record of the evolving *P–T* conditions during growth, especially for crystals > 5 mm (Caddick et al., 2010). Garnet cores have p(Gr_s) contents of 0.18 – 0.19, which is predicted at the garnet-in line at 3.5 – 4.5 kbar and 520 °C. The decrease in p(Gr_s) during progressive growth into garnet + staurolite-bearing assemblages supports a clockwise *P–T* trajectory. Although the Ca zoning does not require an increase in pressure with increasing temperature, the peak assemblage is interpreted to contain garnet and staurolite in the absence of chlorite, which occurs above 4.8 kbar at 575–680 °C. Garnet rims have p(Gr_s) values from 0.09 to 0.06, which provide a minimum estimate for peak conditions between 575 and 610 °C at 4.8 – 5.8 kbar (approximated by the p(Gr_s) contour of 0.08; Fig. 5).

Garnet and staurolite porphyroblasts are interpreted to have grown during the development of the foliation under peak metamorphic conditions. In situ Lu–Hf dates of garnet cores and rims from this sample yield an isochron age of c. 559 Ma (GSWA 210670, preliminary data). Monazite grains that are aligned with this fabric yield a date of 502 ± 3 Ma, interpreted as the timing of peak metamorphism and deformation (Fielding et al., 2019b). Two additional samples collected within the Billyarra Shear Zone have similar assemblages and record similar monazite dates (Fielding et al., 2019a,c). These results demonstrate that the Billyarra Shear Zone was active at 510–500 Ma, reaching peak metamorphic conditions above 575 °C and 4.8 kbar by c. 559 Ma. The rotation of garnet grains during growth and the development of a pervasive foliation at peak metamorphic conditions is consistent with synchronous metamorphism and deformation.

Peak metamorphic conditions are estimated above 575 °C and 4.8 kbar, with a maximum apparent thermal gradient of 120 °C/kbar. The mineral assemblage evolution and garnet compositions are most consistent with a clockwise prograde *P–T* trajectory.

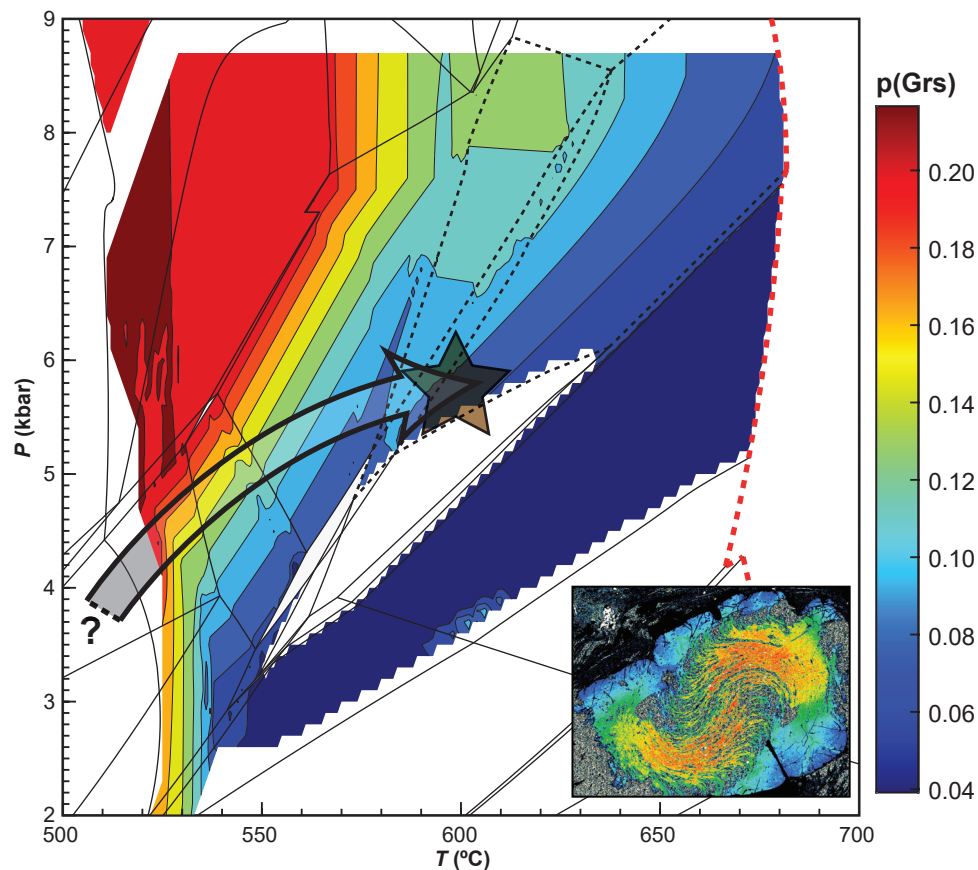


Figure 5. Calcium content — as p(Grs) — for garnet porphyroblast in sample 210670: staurolite-bearing garnet pelitic schist, Lennard River (see Figure 4 for labelled P - T diagram). The garnet zoning is consistent with prograde growth, and the peak assemblage of garnet–staurolite–biotite–muscovite–magnetite–ilmenite–quartz with the garnet rim compositions indicate peak conditions above 5 kbar and 575 °C. Schematic P - T path is represented by the grey arrow, with thickness of the arrow to qualitatively depict uncertainty; star denotes minimum peak conditions. Inset shows Ca map for garnet porphyroblast shown on Figure 2 (see Appendix 2); colours between compositional map and contours are comparable

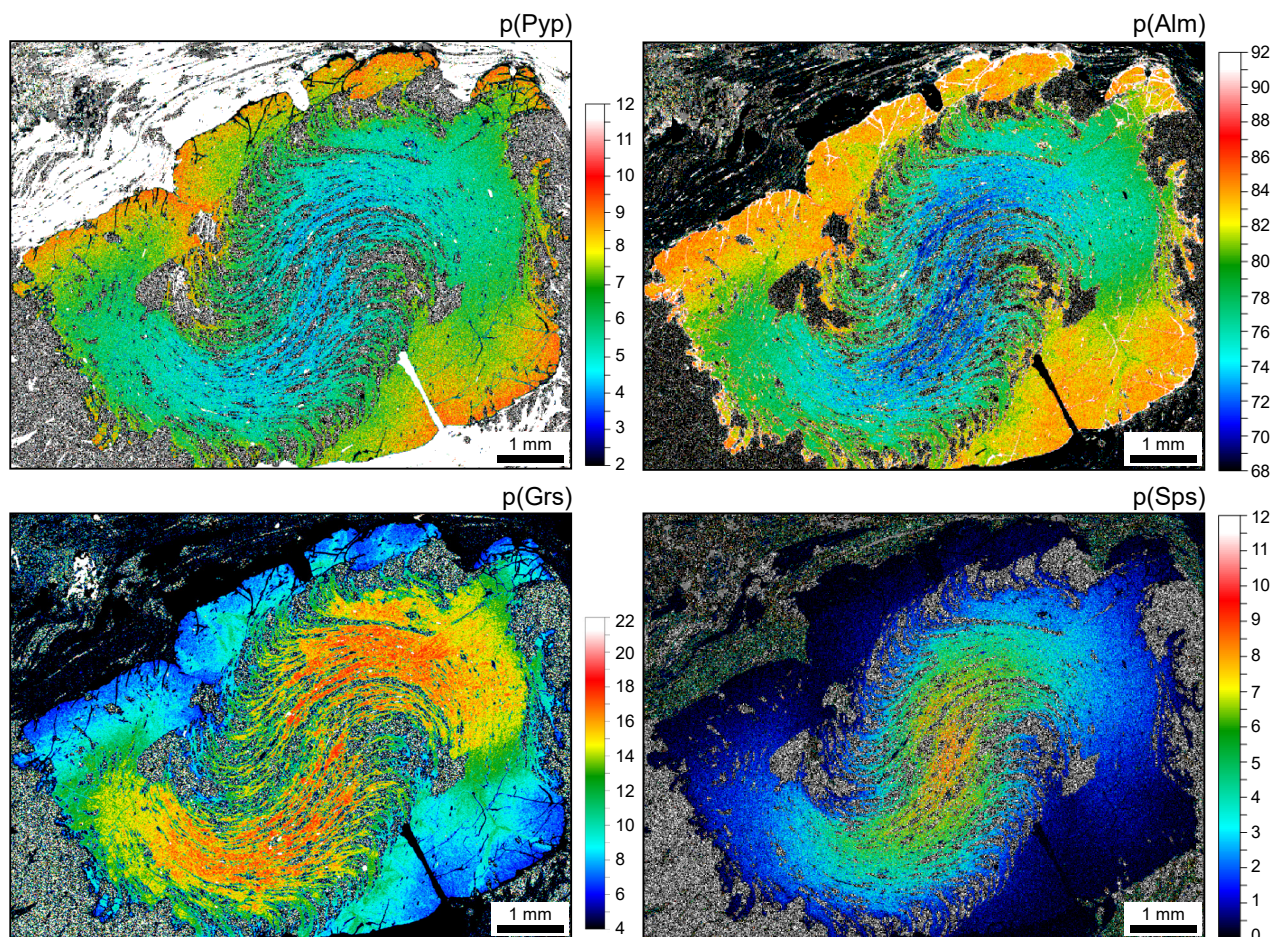
References

- Caddick, MJ, Konopásek, J and Thompson, AB 2010, Preservation of garnet growth zoning and the duration of prograde metamorphism: *Journal of Petrology*, v. 51, no. 11, p. 2327–2347.
- Carlson, WD 2006, Rates of Fe, Mg, Mn, and Ca diffusion in garnet: *American Mineralogist*, v. 91, no. 1, p. 1–11.
- Fielding, IOH, Wingate, MTD, Lu, Y, Korhonen, FJ and Hollis, JA 2019a, 210664: pelitic schist, Lennard River; *Geochronology Record* 1617: Geological Survey of Western Australia, 5p.
- Fielding, IOH, Wingate, MTD, Lu, Y, Korhonen, FJ and Hollis, JA 2019b, 210670: pelitic schist, Lennard River; *Geochronology Record* 1618: Geological Survey of Western Australia, 8p.
- Fielding, IOH, Wingate, MTD, Lu, Y, Korhonen, FJ and Hollis, JA 2019c, 210671: pelitic schist, Lennard River; *Geochronology Record* 1619: Geological Survey of Western Australia, 6p.
- Holland, TJB and Powell, R 2011, An improved and extended internally consistent thermodynamic dataset for phases of petrological interest, involving a new equation of state for solids: *Journal of Metamorphic Geology*, v. 29, no. 3, p. 333–383.
- Korhonen, FJ, Kelsey, DE, Fielding IOH and Romano, SS 2020, The utility of the metamorphic rock record: constraining the pressure–temperature–time conditions of metamorphism: *Geological Survey of Western Australia, Record* 2020/14, 24p.
- Lu, Y, Wingate, MTD, Kirkland, CL, Maidment, DW, Phillips, C and Hollis, JA 2016, 212344: pelitic schist, Napier Creek; *Geochronology Record* 1348: Geological Survey of Western Australia, 6p.
- Maidment, DW, Lu, Y, Phillips, C, Korhonen, FJ, Fielding, IOH, Wingate, MTD, Kirkland, CL, Murphy, R, Tilhac, R, Poujol, M and Zhao, J 2022, *Geochronology of metasedimentary and igneous rocks in the Lamboo Province, Kimberley region: reassessing collisional geodynamic models*: Geological Survey of Western Australia, Report 215, 89p.
- Palin, RM, White, RW and Green, ECR 2016, Partial melting of metabasic rocks and the generation of tonalitic-trondhjemitic-granodioritic (TTG) crust in the Archaean: Constraints from phase equilibrium modelling: *Precambrian Research*, v. 287, p. 73–90, doi:10.1016/j.precamres.2016.11.001.
- Pearce, MA, White, AJR and Gazley, MF 2015, TCInvestigator: automated calculation of mineral mode and composition contours for thermocalc pseudosections: *Journal of Metamorphic Geology*, v. 33, no. 4, p. 413–425, doi:10.1111/jmg.12126.

- Powell, R and Holland, TJB 1988, An internally consistent dataset with uncertainties and correlations: 3. Applications to geobarometry, worked examples and a computer program: *Journal of Metamorphic Geology*, v. 6, no. 2, p. 173–204.
- Shaw, RD, Tyler, IM, Griffin, TJ and Webb, A 1992, New K–Ar constraints on the onset of subsidence in the Canning Basin, Western Australia: *BMR Journal of Geology and Geophysics*, v. 13, p. 31–35.
- Tyler, IM and Griffin, TJ 1990, Structural development of the King Leopold Orogen, Kimberley region, Western Australia: *Journal of Structural Geology*, v. 12, p. 703–714.
- Tyler, IM, Hocking, RM and Haines, PW 2012, Geological evolution of the Kimberley region of Western Australia: *Episodes* v. 35, p. 298–306.
- Tyler, IM, Page, RW and Griffin, TJ 1999, Depositional age and provenance of the Marboo Formation from SHRIMP U–Pb zircon geochronology: implications for the early Palaeoproterozoic tectonic evolution of the Kimberley region, Western Australia: *Precambrian Research*, v. 95, p. 225–243.
- White, RW, Powell, R, Holland, TJB, Johnson, TE and Green, ECR 2014a, New mineral activity-composition relations for thermodynamic calculations in metapelitic systems: *Journal of Metamorphic Geology*, v. 32, no. 3, p. 261–286.
- White, RW, Powell, R and Johnson, TE 2014b, The effect of Mn on mineral stability in metapelites revisited: New a–x relations for manganese-bearing minerals: *Journal of Metamorphic Geology*, v. 32, no. 8, p. 809–828.

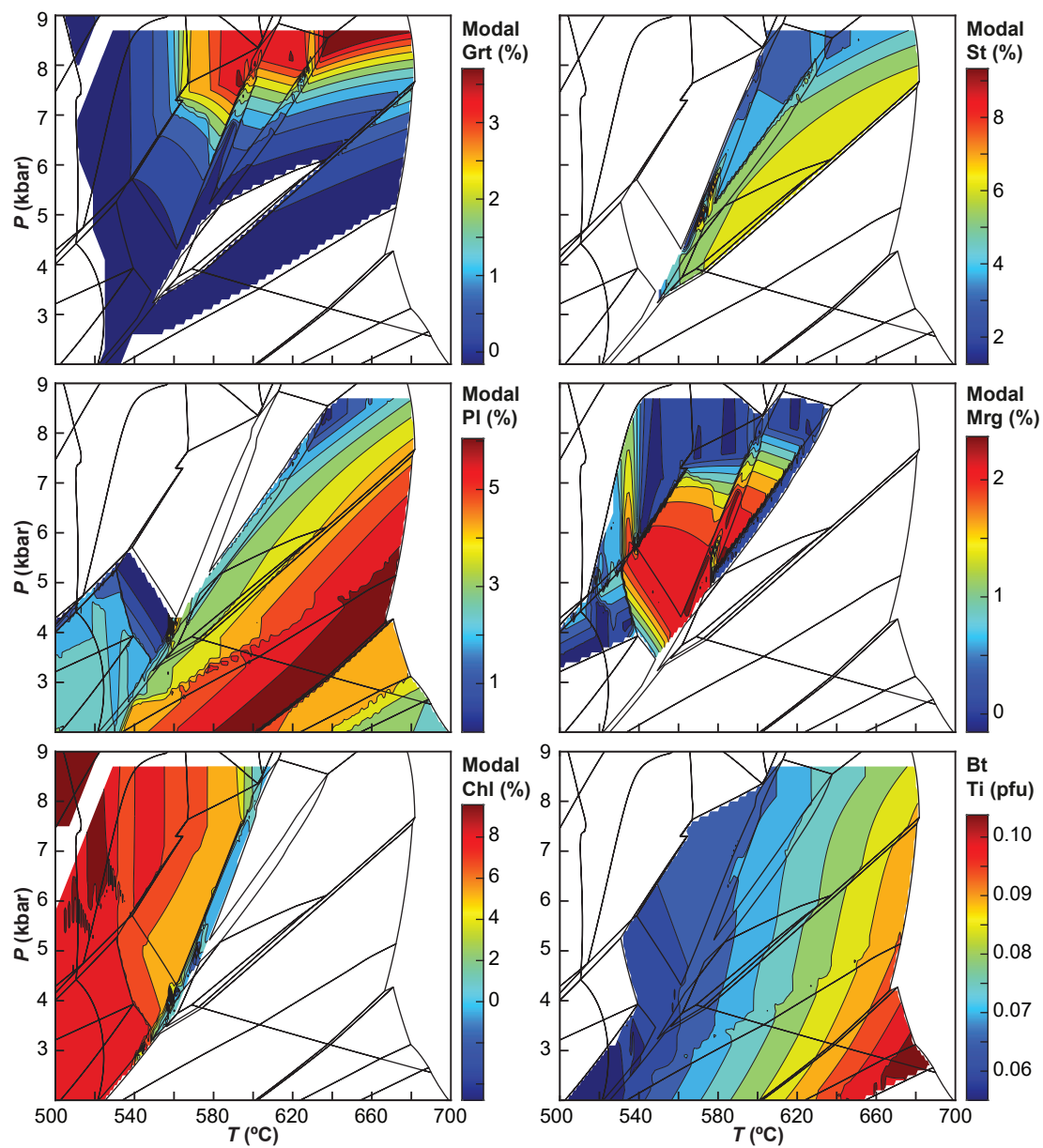
Appendix 2

Quantitative EPMA compositional maps of a garnet grain in sample 210670: staurolite-bearing garnet pelitic schist, Lennard River, calculated for proportion of garnet end-members. The analysed garnet grain is identified in Figure 2. Abbreviations: Prp, pyrope; Alm, Almandine; Grs, grossular; Sps, spessartine



Appendix 3

Mode (mineral proportions; approximately equal to volume percent) and compositional isopleths for selected minerals in sample 210670: staurolite-bearing garnet pelitic schist, Lennard River. Labelled P - T diagram provided in Figure 4



Links

[Record 2020/14 The utility of the metamorphic rock record: constraining the pressure–temperature–time conditions of metamorphism](#)

[Appendix 1](#) (an accompanying electronic file on eBookshop)

Recommended reference for this publication

Korhonen, FJ, Romano, SS, Fielding, IOH, Kelsey, DE and Hollis, JA 2022, 210670: staurolite-bearing garnet pelitic schist, Lennard River; Metamorphic History Record 25: Geological Survey of Western Australia, 8p.

Data obtained: 6 November 2018

Date released: 7 October 2022

This Metamorphic History Record was last modified on 5 October 2022

Grid references in this publication refer to the Geocentric Datum of Australia 1994 (GDA94). All locations are quoted to at least the nearest 100 m.

WAROX is GSWA's field observation and sample database. WAROX site IDs have the format 'ABCXXXnnnnnnSS', where ABC = geologist username, XXX = project or map code, nnnnnn = 6 digit site number, and SS = optional alphabetic suffix (maximum 2 characters).

Isotope and element analyses are routinely conducted using the GeoHistory laser ablation ICP-MS and Sensitive High-Resolution Ion Microprobe (SHRIMP) ion microprobe facilities at the John de Laeter Centre (JdLC), Curtin University, with the financial support of the Australian Research Council and AuScope National Collaborative Research Infrastructure Strategy (NCRIS). The TESCAN Integrated Mineral Analyser (TIMA) instrument was funded by a grant from the Australian Research Council (LE140100150) and is operated by the JdLC with the support of the Geological Survey of Western Australia, The University of Western Australia (UWA) and Murdoch University. Mineral analyses are routinely obtained using the electron probe microanalyser (EPMA) facilities at the Centre for Microscopy, Characterisation and Analysis, UWA, at Adelaide Microscopy, University of Adelaide, and at the Electron Microscopy and X-ray Microanalysis Facility, University of Tasmania.

Digital data related to WA Geology Online, including geochronology and digital geology, are available online at the Department's [Data and Software Centre](#) and may be viewed in map context at [GeoVIEW.WA](#).

Disclaimer

This product uses information from various sources. The Department of Mines, Industry Regulation and Safety (DMIRS) and the State cannot guarantee the accuracy, currency or completeness of the information. Neither the department nor the State of Western Australia nor any employee or agent of the department shall be responsible or liable for any loss, damage or injury arising from the use of or reliance on any information, data or advice (including incomplete, out of date, incorrect, inaccurate or misleading information, data or advice) expressed or implied in, or coming from, this publication or incorporated into it by reference, by any person whosoever.



© State of Western Australia (Department of Mines, Industry Regulation and Safety) 2022

With the exception of the Western Australian Coat of Arms and other logos, and where otherwise noted, these data are provided under a Creative Commons Attribution 4.0 International Licence. (<http://creativecommons.org/licenses/by/4.0/legalcode>)

Further details of geoscience products are available from:

Information Centre
Department of Mines, Industry Regulation and Safety
100 Plain Street
EAST PERTH WA 6004
Telephone: +61 8 9222 3459 | Email: publications@dmirs.wa.gov.au
www.dmirs.wa.gov.au/GSWApublications